





## ORIGINAL ARTICLE

# Dynamic three-dimensional computed tomographic imaging facilitates evaluation of the equine cervical articular process joint in motion

Nicole Schulze<sup>1</sup>  | Natasha Werpy<sup>2</sup> | Jennifer Gernhardt<sup>1</sup> | Guido Fritsch<sup>3</sup> | Thomas Hildebrandt<sup>3</sup> | Katrien Vanderperren<sup>4</sup> | Robert Klopffleisch<sup>5</sup>  | Racem Ben Romdhane<sup>6</sup>  | Christophorus Lischer<sup>1</sup> | Anna Ehrle<sup>1</sup> 

<sup>1</sup>Equine Clinic, Surgery and Radiology, Freie Universität Berlin, Berlin, Germany

<sup>2</sup>Equine Diagnostic Imaging Inc., Archer, Florida, USA

<sup>3</sup>Leibniz Institute for Zoo and Wildlife Research, Forschungsverbund Berlin e.V., Berlin, Germany

<sup>4</sup>Department of Veterinary Medical Imaging and Small Animal Orthopaedics, Ghent University, Ghent, Belgium

<sup>5</sup>Institute for Veterinary Pathology, Freie Universität Berlin, Berlin, Germany

<sup>6</sup>Institute for Veterinary Epidemiology and Biostatistics, Freie Universität Berlin, Berlin, Germany

## Correspondence

Nicole Schulze, Equine Clinic, Surgery and Radiology, Freie Universität Berlin, Berlin, Germany.

Email: [nicole.schulze@fu-berlin.de](mailto:nicole.schulze@fu-berlin.de)

## Funding information

European College of Veterinary Surgeons (ECVS Residents Research Grant).

## Summary

**Background:** Dynamic computed tomography (CT) imaging has been introduced in human orthopaedics and is continuing to gain popularity. With dynamic CT, video sequences of anatomical structures can be evaluated in motion.

**Objectives:** To investigate the feasibility of dynamic CT for diagnostic imaging of the equine cervical articular process joints (APJs) and to give a detailed description of the APJ movement pattern.

**Study design:** Descriptive cadaver imaging.

**Methods:** Cervical specimens of twelve Warmblood horses were included. A custom-made motorised testing device was used to position and manipulate the neck specimens and perform dynamic 2D and 3D CT imaging. Images were obtained with a 320-detector-row CT scanner with a 160 mm wide-area (2D) solid-state detector design that allows image acquisition of a volumetric axial length of 160 mm without moving the CT couch. Dynamic videos were acquired and divided into four phases of movement. Three blinded observers used a subjective scale of 1 (excellent) to 4 (poor) to grade the overall image quality in each phases of motion cycle.

**Results:** With an overall median score of 1 the image quality, a significantly lower score was observed in the dynamic 3D videos over the four phases by the three observers compared with the 2D videos for both flexion (3D 95% CI: 1-2 and 2D 95% CI: 1-3;  $P = .007$ ) and extension movement (3D 95% CI: 1-2 and 2D 95% CI: 1-3;  $P = .008$ ). Median Translational displacement of the APJ surface was significantly greater in flexion than in extension movement ( $P = .002$ ).

**Main limitations:** The small number of specimens included. Excision of spines and removal of musculature.

**Conclusions:** The study is a first step in the investigation of the potential of dynamic 3D CT in veterinary medicine, a technique that has only begun to be explored and leaves much room for refinement prior to its introduction in routine practice. CT with

This is an open access article under the terms of the [Creative Commons Attribution](https://creativecommons.org/licenses/by/4.0/) License, which permits use, distribution and reproduction in any medium, provided the original work is properly cited.

© 2022 The Authors. *Equine Veterinary Journal* published by John Wiley & Sons Ltd on behalf of EVJ Ltd.

a detector coverage of 16 cm and a rotation speed of 0.32 seconds provides high-quality images of moving objects and gives new insight into the movement pattern of equine cervical APJs.

#### KEYWORDS

articular process joints, cervical spine, dynamic computed tomography, horse, image quality

## 1 | INTRODUCTION

Three-dimensional (3D) reconstruction of computed tomographic (CT) images can be used in presurgical planning and has other applications in veterinary patients.<sup>1</sup> Dynamic CT imaging has been introduced in human orthopaedics over the past decade and is continuing to gain popularity, but the technique is not yet utilised in veterinary medicine.<sup>2,3</sup> With dynamic CT, anatomical structures can be evaluated in motion as multiple image volumes are recorded over time and subsequently reviewed in form of a video sequence.<sup>4</sup> The acquired dataset can be examined either as a dynamic 3D volume-rendered view (dynamic 3D CT) or a dynamic 2D cross-section in any imaging plane (dynamic 2D CT).<sup>5</sup>

The application of dynamic 3D CT is of interest, especially for the investigation of musculoskeletal diseases with a dynamic component like bone impingement, intra-articular ligament sufficiency, dynamic instability syndromes and dynamic vascular compression in man.<sup>6-8</sup> Several studies have demonstrated the potential of dynamic 3D CT for the evaluation of the human wrist, shoulder, knee and hip in motion.<sup>8-13</sup>

The cervical spine and particularly the articular process joints (APJs) are currently receiving increased attention as a source of dysfunction in the equine patient.<sup>14-19</sup> The range of motion (ROM) of the cervical spine has major implications for the coordination and balance of the equine locomotor system and the availability of large CT gantry apertures in several equine referral centres makes detailed multidimensional diagnostic imaging of the equine cervical spine more applicable.<sup>19-22</sup> Whilst there are some studies detailing the CT anatomy as well as pathological findings in the equine cervical spine, little is known about the exact interaction, movement pattern and ROM of the cervical APJs during dorsoventral flexion-extension and lateral bending.<sup>23-25</sup>

Pathological conditions of the equine cervical APJs include osteochondrosis, fracture and degenerative joint disease.<sup>26-28</sup> Although associated imaging findings may be incidental, pathology of the equine cervical APJs can also result in cervical nerve root and spinal cord compression leading to clinical signs such as decreased cervical ROM, lameness and ataxia.<sup>16,23,27,29-32</sup> Pathology in the equine cervical spine commonly involves a dynamic component. Therefore, assessment of affected segments in motion has the potential to aid the detection of dynamic stenotic conditions.

The aim of this study was to investigate the feasibility of dynamic CT for diagnostic imaging of the equine cervical APJs and to give a detailed description of APJ movement in a cadaver model. We hypothesised that dynamic CT facilitates the comprehensive assessment of the equine cervical APJ components in motion.

## 2 | MATERIALS AND METHODS

### 2.1 | Neck specimens

Cervical specimens ( $n = 12$ ) were collected from Warmblood horses without evidence of cervical pathology, humanely destroyed for reasons unrelated to this study. Horses were between 3 and 31 years of age (mean = 12 years) and included six geldings and six mares. This sampling protocol was adopted to comply with the exploratory nature of this study and with animal welfare considerations.

Specimens were excised at the atlantooccipital joint and at the cervicothoracic junction.<sup>24</sup> The perivertebral musculature including the intertransversarii cervicis and longus colli muscles and the joint capsules were left intact. Specimens were frozen at  $-20^{\circ}\text{C}$  immediately after dissection and subsequently thawed over 24 hours at  $10^{\circ}\text{C}$  prior to biomechanical testing.

### 2.2 | Testing device

Based on a previous protocol, a custom-made motorised testing device was used to position and manipulate the neck specimens to perform dynamic computed tomographic (dynamic 2D and 3D CT) imaging (Figure 1).<sup>24</sup> The testing device provided consistent and controlled movement of the APJ

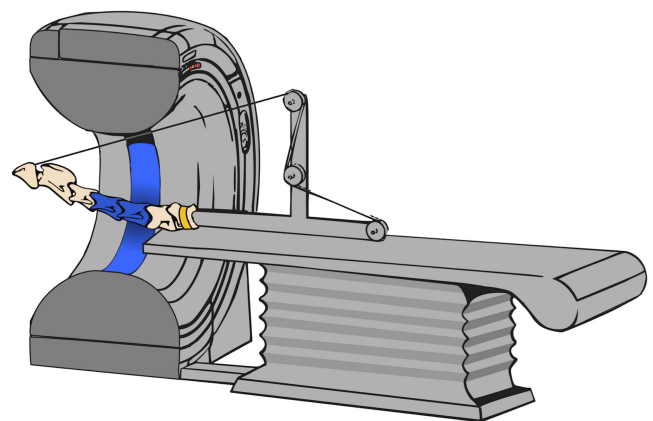


**FIGURE 1** Custom-made motorised device for biomechanical testing of equine neck specimens ( $C_1$ - $C_7$ ). A specimen is illustrated in neutral position for computed tomographic (CT) imaging (320-detector-row CT scanner, Aquilion One, Canon Medical Systems) of the motion segment  $C_{4/5}$  (field of view indicated in blue). The body of  $C_7$  is fixed in the device (yellow band).  $C_1$  is secured to a rope, leading through a pulley system and attached to a rope winch

in flexion and extension. The vertebral body of  $C_7$  was fixed in the device and  $C_1$  was attached to a rope which led through a pulley and was connected to a rope winch. Additionally, a wooden frame was used to support the weight of the specimen during motion. The motion segment  $C_{4/5}$  was evaluated in this study. The two motion segments ( $C_{5/6}$  and  $C_{6/7}$ ) caudal to the motion segment of interest ( $C_{4/5}$ ) were not attached to the frame, to allow full ROM of these adjacent segments. The applied force was standardised and limited to 50 Nm and the speed to 0.05 m/seconds.<sup>33</sup>

### 2.3 | Computed tomographic imaging

Computed tomographic imaging was performed using an intermittent sequential mode with a 320 detector row CT scanner with a 160 mm wide-area (2D) solid-state detector design that allows image acquisition of a volumetric axial length of 160 mm without moving the CT couch (Aquilion One; Canon Medical Systems). The gantry opening was 78 cm. A field-of-view of 50 cm with  $512 \times 512$  pixels, 0.5 mm slice thickness and a tube rotation time of 0.35 seconds at 100 kVp and 280 mAs (100 effective mAs) were used. Supplementary videos illustrate the CT data (Videos S1-S4): Two dynamic CT scans including full range of extension (Video S1) and flexion (Video S3) and were performed on each neck specimen with focus on the motion segment  $C_{4/5}$ .

### 2.4 | Computed tomography analysis

The movement of each cervical spine segment ( $C_{4/5}$ ) was viewed in three planes using multiplanar reconstruction (MPR) mode (dynamic 2D

CT) (Figure 2). Sagittal plane images were exported as 2D videos (Videos S1 and S3) as well as dynamic 3D reconstructions (volume rendering) (Videos S2 and S4 and Figure 3). Prior to further evaluation, images were screened for the presence of pathological changes and specimens with evidence of cervical spine pathology were not included in the trial.

For the assessment of the overall image quality and presence of motion artefacts, the dynamic 2D and dynamic 3D videos were divided into four phases of movement. Phases were equally long, with 2-4 seconds per phase depending on the total length of the motion cycle (maximum length 14 seconds). A subjective scale of 1-4 (1 = excellent, no motion artefacts; 2 = good, subtle motion artefacts; 3 = fair, moderate motion artefacts, evaluation possible and 4 = poor, severe motion artefacts, evaluation not possible) was used to grade the overall image quality in each of the four phases (Figure 4). The overall image quality of all four phases was additionally evaluated based on the same score.

Images were blinded and analysed independently by a board-certified veterinary radiologist (KV), a board-certified veterinary surgeon (AE) and a third-year equine surgery resident (NS) using open-source imaging software with three-dimensional multiplanar reconstruction (MPR) capability (Horos 64-bit DICOM viewer, Horos Project, 2015) on an image analysis workstation (Apple iMac Pro 2017). The sum of scores attributed by each observer for each of the four phases of movement was used to assess the intra- and inter-observer agreement. The intra-observer agreement was determined by evaluating all images twice within one month (NS) and the evaluation of the inter-observer agreement was based on a comparison of the three observers (KV, AE, NS).

For the analysis of the APJ movement pattern, three images were selected for each  $C_{4/5}$  motion segment, one with the cervical spine in a neutral position, one in maximal flexion and one in maximal

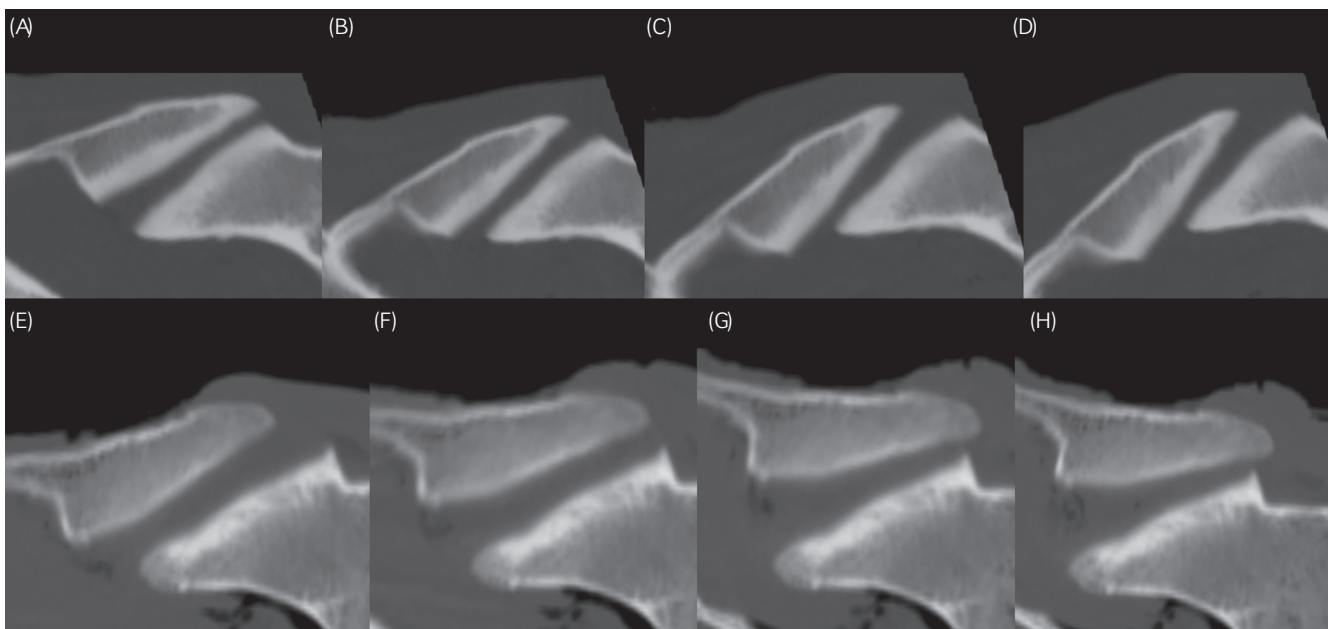


**FIGURE 2** Following computer tomographic evaluation, dynamic 2D sagittal plane videos of the  $C_{4/5}$  motion segment were divided into four phases of movement. Starting at the neutral position (A), 2D captures of initial (B), mid- (C) and full-flexion (D) as well as neutral position (E) initial (F), mid- (G) and full-extension (H) are shown. The four phases of each motion cycle were assessed for overall image quality and presence of motion artefacts

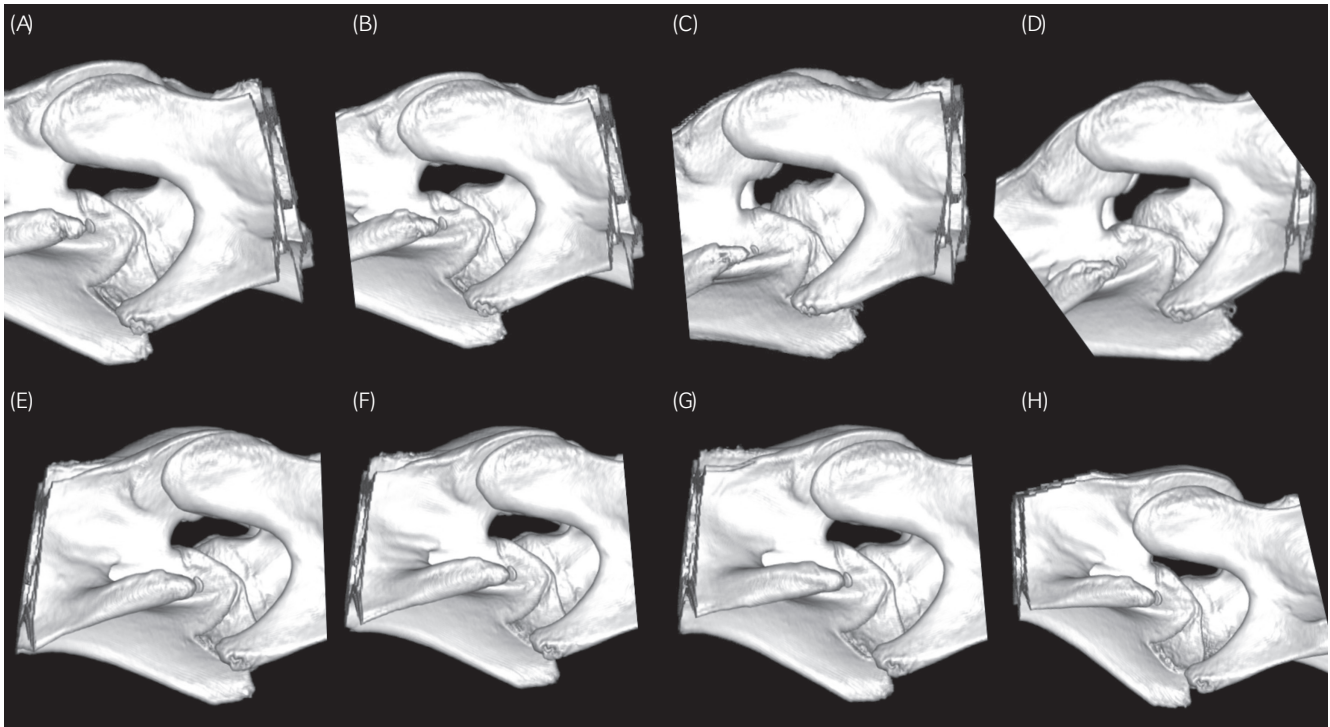
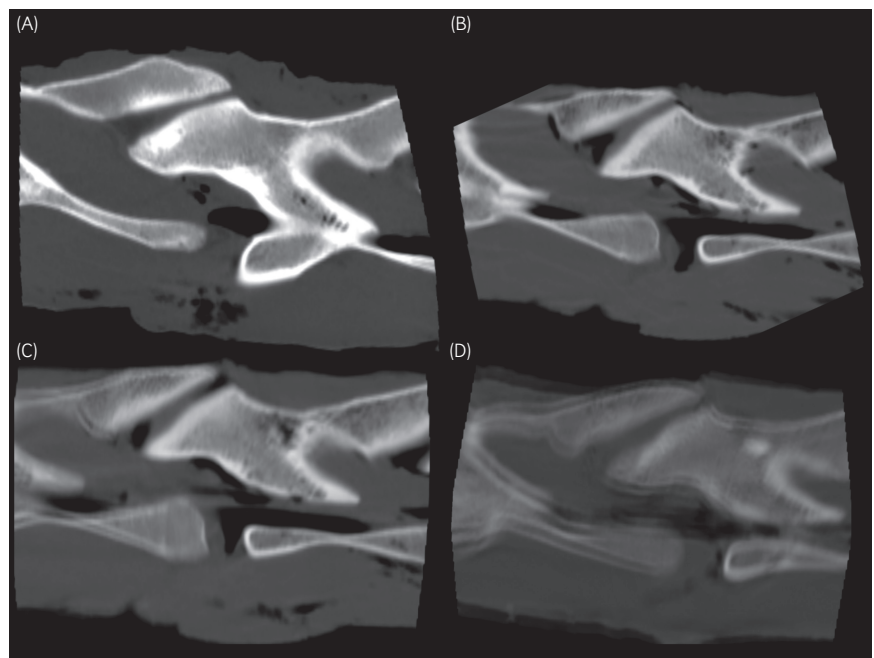


**FIGURE 3** Sagittal plane computer tomographic images were exported as dynamic 3D reconstructions (volume rendering). The dynamic 3D videos of the  $C_{4/5}$  motion segment were split into four phases of flexion (A-D) and extension (E-H) movement and graded to describe the presence of motion artefacts and the image quality

**FIGURE 4** Four phases of a movement cycle (flexion and extension) were assessed based on video sequences (2D and 3D) of the dynamic computer tomographic evaluation of the  $C_{4/5}$  motion segment of 12 equine cervical spine specimens. The presence of motion artefacts and the overall image quality were subjectively graded as 1 = excellent, no motion artefacts (A); 2 = good, subtle motion artefacts (B); 3 = fair, moderate motion artefacts, evaluation possible (C) and 4 = poor, severe motion artefacts, evaluation not possible (D) by three-blinded observers



extension. The neutral position was defined as the point at which the caudal aspect of the cranial articular process of  $C_5$  and the caudal aspect of the caudal articular process of  $C_4$  were superimposed. In flexion, the cranial translational displacement of the caudal articular process of  $C_4$  relative to the cranial articular process of  $C_5$  was measured. In extension, the caudal translational displacement of the caudal articular process of  $C_4$  compared with the cranial articular process of  $C_5$  was determined (Figure 5).

## 2.5 | Data analysis

Data were recorded in Excel (Microsoft Inc) and analysed in SPSS (IBM® SPSS® Statistics). Data were visually assessed and found not to be normally distributed and analysed using the Wilcoxon signed-rank test for pairwise comparison to compare the difference of translation in flexion vs. extension movements and the difference between the right and left translations both in flexion and extension

movements. The intra-observer agreement was assessed using the Wilcoxon Signed Rank Test and the inter-observer agreement was determined using the Friedman test. For all tests, a *P*-value of <.05 was considered statistically significant. A Bonferroni correction was applied to the significance threshold when relevant.

### 3 | RESULTS

#### 3.1 | Dynamic 2D image quality and artefacts

In flexion, the median image quality of the dynamic 2D imaging was rated with a score of 2 (95% CI: 1-3) in phase II. Subtle motion artefacts were visible but did not impact on the image evaluation. Flexion phases I, III and IV (95% CI: 1-3.05, 1-3 and 1-1.05, respectively) were graded with a score of 1 without evidence for motion artefacts. In extension, the median image quality was graded with an average score of 1.5 in phases I and II (95% CI: 1-3.05 both). Phases III and IV were rated with 1 (95% CI: 1-2.05 and 1-2, respectively). The median overall image quality of all four phases was 1 in flexion and extension (95% CI: 1-3 both).

#### 3.2 | Dynamic 3D image quality and artefacts

For the dynamic 3D videos, all raters gave excellent scores (1) for phases I-IV in flexion and extension. The median overall image quality of all four phases was also rated as 1 in flexion and extension.

#### 3.3 | Dynamic 2D vs. dynamic 3D image quality

The image quality of the dynamic 3D videos was significantly better when compared with the dynamic 2D videos in flexion and

extension. A significantly lower score was observed in the dynamic 3D videos over the four phases by the three observers for both flexion (95% CI: 1-2 and 1-3, respectively for 3D and 2D videos; *P* =.007) and extension movement (95% CI: 1-2 and 1-3, respectively for 3D and 2D videos; *P* =.008).

#### 3.4 | Intra- and interobserver agreement

No significant intra-observer difference (dynamic 2D flexion 95% CI: 4-7.73 vs 4.28-8, *P* =.8; dynamic 2D extension 95% CI: 4-9.5 vs 4-9.7, *P* =.4; dynamic 3D flexion 95% CI: 4-6 vs 4-6, *P* = 1; dynamic 3D extension 95% CI: 4-5 vs 4-5.73, *P* =.4) was detected between the two summed scores attributed by the same observer (NS) for the studied movements (flexion and extension) in both 2D and 3D videos at different time points. A significant inter-observer difference was evident between the summed scores given by the three observers for the 2D videos for both the flexion (95% CI: 4-7.73, 4-8.73 and 4-6.73, respectively, for the three observers, *P* =.001) and extension (95% CI: 4-9.45, 4-9.9 and 4-6.73, respectively, for the three observers, *P* =.009) movement. Good inter-observer agreement was found for the assessment of dynamic 3D videos for flexion (95% CI: 4-6, 4-6 and 4-5.73, respectively, for the three observers, *P* =.9) and extension (95% CI: 4-5, 4-7.45 and 4-6, respectively, for the three observers, *P* =.6).

#### 3.5 | Translational displacement of the APJ surfaces

The median length of the cranial and caudal APJ surface was 43.57 mm. In flexion, the median displacement of the caudal APJ surface of  $C_4$  relative to the cranial APJ surface of  $C_5$  was 18.79 mm towards cranial for the left side and 17.22 mm for the right side

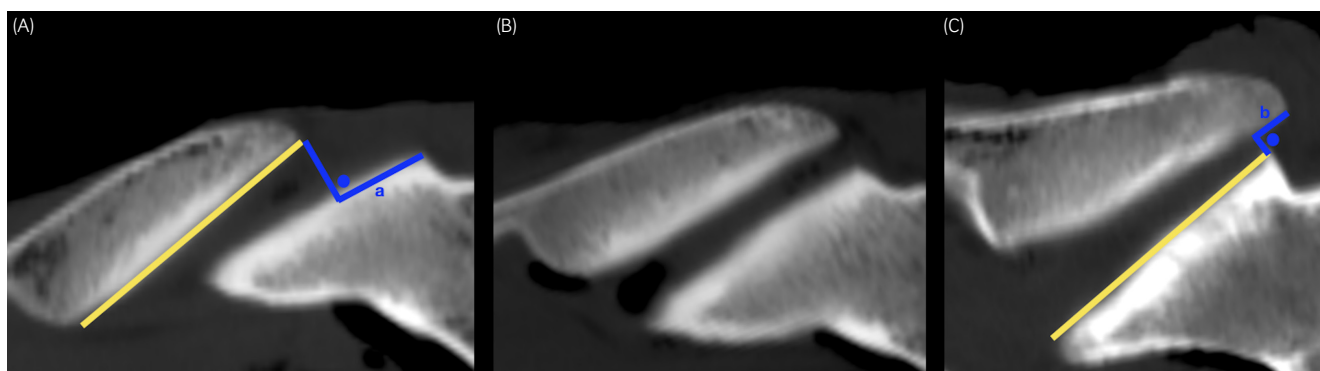


**FIGURE 5** (A) Two-dimensional sagittal plane computer tomographic (CT) image of  $C_{4/5}$  in maximal flexion. The translational displacement of the caudal articular process joint (APJ) surface of  $C_4$  against the cranial APJ surface of  $C_5$  towards cranial was measured as indicated. yellow line = length of the caudal APJ surface of  $C_4$ ; blue right angle = translational displacement in flexion (a). (B) Two-dimensional sagittal plane CT image of  $C_{4/5}$  in neutral position with the caudal aspect of the APJ surface of  $C_4$  and  $C_5$  superimposed. (C) Two-dimensional sagittal plane CT image of  $C_{4/5}$  in maximal extension. The translational displacement of the caudal APJ surface of  $C_4$  against the cranial APJ surface of  $C_5$  towards caudal was determined as shown. yellow line = length of the cranial APJ surface of  $C_5$ ; blue right angle = translational displacement in extension (b)

(Figure 5A). In extension, the median displacement of the caudal APJ surface of C<sub>4</sub> relative to the cranial APJ surface of C<sub>5</sub> was 2.78 mm towards caudal for the left side and 1.82 mm for the right side (Figure 5C). There was no statistically significant difference in the displacement of the APJs between the left and right sides of the flexion (95% CI: 12.78-23.00 and 12.00-21.87, respectively, for left and right sides; *P* = .5) and extension (95% CI: 1.21-6.04 and 0-8.26, respectively for left and right sides; *P* = .3) However, significantly more translational displacement was evident in flexion when compared with extension (*P* = .002 for both the right and the left sides).

## 4 | DISCUSSION

The results of this study confirm the feasibility of dynamic 2D and 3D CT for the assessment of the equine cervical APJs based on a cadaver model. Additionally, the investigation gives new insight in the dynamics of the APJ articular components during motion.

Blinded evaluation of 2D and 3D video sequences derived from sagittal plane CT data focused on the motion segment C<sub>4/5</sub> identified an excellent overall image quality for both, flexion and extension movement. During dynamic 2D CT imaging, there was evidence of slight motion artefacts adjacent to the APJs in movement phases I and II in flexion and extension. Most artefacts were observed in the vicinity of the APJs as the soft tissues showed a higher velocity of movement than the APJs themselves. Whilst motion artefacts can impair on image analysis and post-processing, it has been demonstrated that the assessment of axial CT sequences is not qualitatively affected by object motion at 0.05 m/seconds.<sup>2</sup> In addition, each dynamic CT study consists of multiple individual axial sequences, at least one of which was always free of motion artefacts and could be used diagnostically for multiplanar reconstruction without restriction.

The volume acquisition speed of the CT is the most important parameter for motion artefact control.<sup>34</sup> The volume acquisition speed depends on the gantry rotation speed and the image reconstruction technique.<sup>35</sup> An exponential decrease in image quality was seen with lower volume acquisition speeds in previous studies.<sup>2,36</sup> Based on these results the highest gantry rotation speed (0.32 seconds per rotation) is recommended when performing dynamic CT examination.<sup>2,36</sup> The speed of motion of the biomechanical testing device further influences the development of motion artefacts.<sup>11</sup> The speed of the vertebral flexion and extension was pre-determined at 0.05 m/seconds.<sup>24</sup> Most likely a slower speed would have resulted in an improved image quality, but also a substantially higher amount of image data as each acquired volume (0.32 seconds) contains 516 images.<sup>37</sup>

The dynamic 3D videos were free of motion artefacts in phases I-IV in flexion and extension in the current study. This observation can be explained by the calculation of the 3D volume from axial 2D slices, which is accompanied by a loss of resolution. In contrast to another study, there was no evidence for band artefacts in the dataset presented here.<sup>38</sup> The wider detector of the CT used (320

detector - row with 160 mm detector width) might mitigate this type of artefact.

Good intra-observer agreement was found for the assessment of dynamic 2D and 3D videos; however, inter-observer agreement was only evident for dynamic 3D but not dynamic 2D video evaluation. This finding is most likely related to the motion artefacts seen in phases I and II of the 2D videos being very subtle.

The dynamic CT data was used to further investigate the detailed movement pattern of the equine cervical APJs. The translational displacement of the APJ articular surfaces was significantly greater in flexion when compared with extension. In flexion, there was a mean displacement of the APJ surface of over 43% in relation to the mean length of the APJ surface with a displacement of only approximately 7% observed during cervical extension. The exact aetiopathogenesis of cervical APJ osteoarthritis and osteochondrosis is yet to be determined.<sup>39-41</sup> Analysis of the dynamic 2D video series of the C<sub>4/5</sub> APJ identified that the cranial margin of C<sub>5</sub> was located in close proximity to the C<sub>4</sub> articular surface in full flexion. Similarly, the caudal margin of C<sub>5</sub> showed what could be interpreted as an area of increased pressure or impingement on the articular surface of C<sub>4</sub> in full extension of the cervical spine, potentially contributing to the development of osteochondrosis or osteoarthritis in this area (Figure 6). In a recent report, osteochondral fragments were identified in 24% of horses with cervical dysfunction.<sup>19</sup> The majority of fragments (19/22) were located within the APJ synovial outpouchings, in either a ventral axial or dorsal abaxial location adjacent to the articular margin.

Besides the described musculoskeletal applications, dynamic CT facilitates radiotherapy planning in human patients.<sup>37</sup> Targeted radiation can be performed in cases with thoracic neoplasia resulting in a reduced chance of a geographic miss due to movement artefacts.<sup>37,42</sup> Dynamic CT angiography is used for visualisation of vascular pathology in the brain and spine and contrast agent enhancement in the heart and pulmonary vessels can be displayed in real time during a cardiac cycle.<sup>37,43,44</sup>

Static CT is an accepted modality in equine orthopaedic advanced diagnostic imaging and an excellent tool for the evaluation of fracture configurations in equine patients.<sup>1,45-47</sup> The ability to display the interaction of articular components during complex movements using dynamic CT additionally facilitates the investigation of potential mechanisms of joint injury. Wide area-detector CT scanners are particularly useful for dynamic studies as they provide high temporal resolution and whole-joint coverage during sequential acquisition.<sup>7</sup> Challenges with the widespread use of dynamic CT in routine diagnostic imaging include the cost of the scanner as well as handling and processing of the large volumetric datasets that are generated using this technique.<sup>37</sup>

In human medicine, the patient is fully conscious and actively performs controlled movements during dynamic CT examination. In veterinary patients, sedation or general anaesthesia is required in order to image controlled movement patterns. In the described investigation, constant and continuous movement of the spinal motion segment C<sub>4/5</sub> was achieved with the aid of a motor-driven external device.<sup>24</sup> Whilst the application of dynamic CT remains technically more demanding

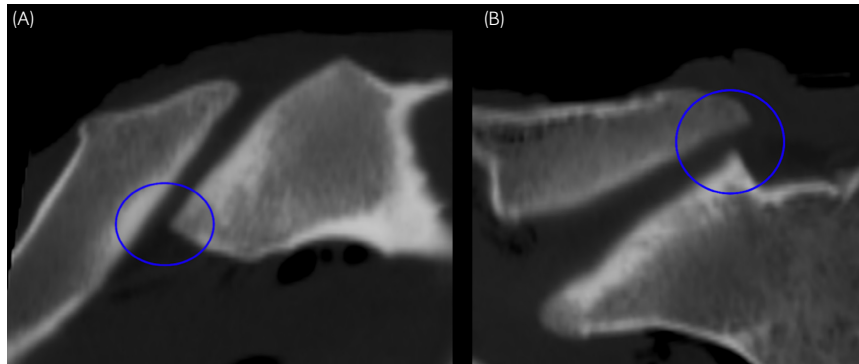


**FIGURE 6** (A) Two-dimensional sagittal plane computer tomographic (CT) image of  $C_{4/5}$  in maximal flexion. Note the close position of the cranial aspect of the cranial articular process of  $C_5$  in relation to the caudal  $C_4$  articular process joint (APJ) surface (blue circle). (B) Two-dimensional sagittal plane CT image of  $C_{4/5}$  in maximal extension. Focused pressure on the caudal margin of the  $C_5$  articular process in this position (blue circle) could relate to an additional predilection site for APJ osteochondrosis and osteoarthritis

in horses when compared with human or small animal patients, the development of similar devices might be useful for the assessment of other regions of the body including the equine distal limb. In humans, however, this CT shows its strength primarily in examinations of anatomical structures in which motion artefacts cannot be avoided (heart and lungs).<sup>37</sup> Recently, the possibility of examining limbs of the standing horse (without general anaesthesia) with high-end fan-beam CT systems was introduced.<sup>48</sup> Since a distal limb of a standing horse can be examined in 0.32 seconds with this system, significantly less influence of motion artefacts can be expected.

Limitations of the described study are the *ex vivo* protocol used and the small number of specimens included. Based on previously described protocols, spines were excised at the level of the atlantooccipital and the cervicothoracic junction with only the perivertebral musculature and the joint capsules left intact.<sup>23,49</sup> Excision might have influenced the mobility of the spine when compared with the ROM of the equine cervical spine in its entirety. Fixation of the cervical spine specimens in the testing device could have additionally impaired on the motion of the APJs. The motion segments adjacent to  $C_{4/5}$  were not attached to the frame to minimise the impact of the construct on the cervical ROM.

The described findings should be interpreted carefully with regard to the exploratory nature of the study. The relatively small sample size and the not randomly selected investigated sample may influence results where non-significant differences were found. Additionally, it may not be valid to draw direct conclusions from the data concerning  $C_{4/5}$  and apply it to other motion segments in the cervical spine as differences in ROM are known to exist particularly towards the cranial cervical spine ( $C_1$ - $C_3$ ). However, the study is a first step to show the potential of dynamic 3D CT in veterinary medicine.

In conclusion, the results of this study confirm that a CT with a detector coverage of 16 cm and a rotation speed of 0.32 seconds makes it possible to obtain high-quality images of equine cervical articular process joint  $C_{4/5}$  in motion. As the acquired dynamic data sets consist of multiple individual volume sets, slight motion artefacts in individual video sequences can be replaced by a different volume for the evaluation of stationary (2D) images. This work further confirms

that dynamic CT imaging has the potential to provide new insight into the movement pattern of articular motion segments, which may be of value for the examination of APJ and other joint conditions. The study provides a first step in the investigation of the potential of dynamic 3D CT in veterinary medicine, a technique that has only begun to be explored and leaves much room for refinement prior to its introduction in routine practice.

#### ACKNOWLEDGEMENTS

We thank the Leibniz Institute for Zoo and Wildlife Research and gratefully acknowledge Alexander Gernhardt for his assistance with the biomechanical testing device and Carola Giersch for 3D illustration of the device. Open access funding enabled and organized by ProjektDEAL.

#### CONFLICT OF INTERESTS

No competing interests have been declared.

#### AUTHOR CONTRIBUTIONS

All authors contributed to the study design and interpretation of the data. N. Schulze, A. Ehrle and N. Werpy were mainly responsible for the planning of the project as well as data acquisition, analysis and interpretation. G. Fritsch, R. Klopffleisch, J. Gernhard, C. Lischer and T. Hildebrandt contributed to the study execution and data analysis. K. Vanderperren and N. Werpy developed the described image analysis and R. Ben Romdhane was mainly responsible for data acquisition and statistical analysis. All authors approved the final version of the manuscript.

#### ETHICAL ANIMAL RESEARCH

Approval for the study was given by the local Committee on Research Ethics.

#### INFORMED CONSENT

Explicit owner informed consent for this study was not obtained but horse owners were made aware that tissues would be used for research in general.

## PEER REVIEW

The peer review history for this article is available at <https://publons.com/publon/10.1111/evj.13560>.

## DATA AVAILABILITY STATEMENT

The data that support the findings of this study are available from the corresponding author upon reasonable request.

## ORCID

Nicole Schulze  <https://orcid.org/0000-0002-1304-5190>

Robert Klopfleisch  <https://orcid.org/0000-0002-6308-0568>

Racem Ben Romdhane  <https://orcid.org/0000-0001-8783-7775>

Anna Ehrle  <https://orcid.org/0000-0001-5338-6195>

## REFERENCES

- Preux M, Klopfenstein Bregger MD, Brünisholz HP, Van der Vekens E, Schweizer-Gorgas D, Koch C, et al. Clinical use of computer-assisted orthopedic surgery in horses. *Vet Surg*. 2020;49:1075–87.
- Gondim Teixeira PA, Formery A-S, Hossu G, Winninger D, Batch T, Gervaise A, et al. Evidence-based recommendations for musculoskeletal kinematic 4D-CT studies using wide area-detector scanners: a phantom study with cadaveric correlation. *Eur Radiol*. 2017;27:437–46.
- Kerkhof FD, Brugman E, D'Agostino P, Dourthe B, van Lenthe GH, Stockmans F, et al. Quantifying thumb opposition kinematics using dynamic computed tomography. *J Biomech*. 2016;49:1994–9.
- White J, Couzens G, Jeffery C. The use of 4D-CT in assessing wrist kinematics and pathology. *Bone Joint J*. 2019;101-B(11):1325–1330.
- Alta TD, Bell SN, Troupis JM, Coghlan JA, Miller D, et al. The new 4-dimensional computed tomographic scanner allows dynamic visualization and measurement of normal acromioclavicular joint motion in an unloaded and loaded condition. *J Comput Assist Tomogr*. 2012;36:749–54.
- Choi YS, Lee YH, Kim S, Cho HW, Song H-T, Suh J-S, et al. Four-dimensional real-time cine images of wrist joint kinematics using dual source CT with minimal time increment scanning. *Yonsei Med J*. 2013;54:1026–32.
- Gondim Teixeira PA, Gervaise A, Louis M, Lecocq S, Raymond A, Aptel S, et al. Musculoskeletal wide detector CT: principles, techniques and applications in clinical practice and research. *Eur J Radiol*. 2015;84:892–900.
- Leng S, Zhao K, Qu M, An K-N, Berger R, McCollough CH, et al. Dynamic CT technique for assessment of wrist joint instabilities. *Med Phys*. 2011;38(Suppl 1):S50.
- Edirisinghe Y, Troupis JM, Patel M, Smith J, Crossett M. Dynamic motion analysis of dart throwers motion visualized through computerized tomography and calculation of the axis of rotation. *J Hand Surg Eur*. 2014;39:364–72.
- Shapeero LG, Dye SF, Lipton MJ, Gould RG, Galvin EG, Genant HK, et al. Functional dynamics of the knee joint by ultrafast, cine-CT. *Invest Radiol*. 1988;23:118–23.
- Tay S-C, Primak AN, Fletcher JG, Schmidt B, Amrami KK, Berger RA, et al. Four-dimensional computed tomographic imaging in the wrist: proof of feasibility in a cadaveric model. *Skeletal Radiol*. 2007;36:1163–9.
- Totterman S, Tamez-Pena J, Kwok E, Strang J, Smith J, Rubens D, et al. 3D visual presentation of shoulder joint motion. *Stud Health Technol Inform*. 1998;50:27–33.
- Wassilew GI, Janz V, Heller MO, Tohtz S, Rogalla P, Hein P, et al. Real time visualization of femoroacetabular impingement and subluxation using 320-slice computed tomography. *J Orthop Res*. 2013;31:275–81.
- Bergmann W, Mik-van Mourik M, Veraa S, Broek J, Wijnberg ID, Back W, et al. Cervical articular process joint osteochondrosis in Warmblood foals. *Equine Vet J*. 2020;52:664–9.
- Dyson SJ. Unexplained forelimb lameness possibly associated with radiculopathy. *Equine Vet Educ*. 2020;32(S10):92–103.
- García-López JM. Neck, back, and pelvic pain in sport horses. *Vet Clin North Am Equine Pract*. 2018;34:235–51.
- Pérez-Nogués M, Vaughan B, Phillips KL, Galuppo LD. Evaluation of the caudal cervical articular process joints by using a needle arthroscope in standing horses. *Vet. Surg*. 2020;49:463–71.
- Thomsen LN, Berg LC, Markussen B, Thomsen PD. Synovial folds in equine articular process joints. *Equine Vet J*. 2013;45:448–53.
- Tucker R, Hall YS, Hughes TK, Parker RA. Osteochondral fragmentation of the cervical articular process joints: prevalence in horses undergoing CT for investigation of cervical dysfunction. *Equine Vet J*. 2020;54:106–13. <https://doi.org/10.1111/evj.13410>
- Puchalski SM. Advances in equine computed tomography and use of contrast media. *Vet Clin North Am Equine Pract*. 2012;28:563–81.
- Wright L, Puchalski SM, Kristoffersen M, Lindegaard C. Arthroscopic approach and intra-articular anatomy of the equine atlanto-occipital joint. *Vet Surg*. 2018;47:756–67.
- Lindgren CM, Wright L, Kristoffersen M, Puchalski SM. Computed tomography and myelography of the equine cervical spine: 180 cases (2013–2018). *Equine Vet Educ*. 2021;33 (9):475–83. <http://dx.doi.org/10.1111/eve.13350>
- Clayton HM, Townsend HG. Kinematics of the cervical spine of the adult horse. *Equine Vet J*. 1989;21:189–92.
- Schulze N, Ehrle A, Weller R, Fritsch G, Gernhardt J, Ben Romdhane R, et al. Computed tomographic evaluation of adjacent segment motion after ex vivo fusion of equine third and fourth cervical vertebrae. *Vet Comp Orthop Traumatol*. 2020;33:1–8.
- Zsoldos RR, Licka TF. The equine neck and its function during movement and locomotion. *Zoology (Jena)*. 2015;118:364–76.
- Pool RR. Difficulties in definition of equine osteochondrosis; differentiation of developmental and acquired lesions. *Equine Vet J*. 1993;25:5–12.
- Powers BE, Stashak TS, Nixon AJ, Yovich JV, Norrdin RW. Pathology of the vertebral column of horses with cervical static stenosis. *Vet Pathol*. 1986;23:392–9.
- Rooney JR. Osteochondrosis in the horse. *Mod Vet Pract*. 1975;56:41–3.
- Dyson SJ. Lesions of the equine neck resulting in lameness or poor performance. *Vet Clin North Am Equine Pract*. 2011;27:417–37.
- Ricardi G, Dyson SJ. Forelimb lameness associated with radiographic abnormalities of the cervical vertebrae. *Equine Vet J*. 1993;25:422–6.
- Stewart RH, Reed SM, Weisbrode SE. Frequency and severity of osteochondrosis in horses with cervical stenotic myelopathy. *Am J Vet Res*. 1991;52:873–9.
- Trostle SS, Dubielzig RR, Beck KA. Examination of frozen cross sections of cervical spinal intersegments in nine horses with cervical vertebral malformation: lesions associated with spinal cord compression. *J Vet Diagn Invest*. 1993;5:423–31.
- Gellman K, Bertram J. The equine nuchal ligament 2: passive dynamic energy exchange in locomotion. *Vet Comp Orthop Traumatol*. 2002;15:7–14.
- Grosjean R, Sauer B, Guerra RM, Blum A, Felblinger J, Hubert J. Degradation of the z-resolution due to a longitudinal motion with a 64-channel CT scanner. *Annu Int Conf IEEE Eng Med Biol Soc*. 2007;2007:4429–32.
- Beeres M, Wichmann JL, Paul J, Mbalisike E, Elsabaie M, Vogl TJ, et al. CT chest and gantry rotation time: does the rotation time influence image quality? *Acta Radiol*. 2015;56:950–4.
- Dawson P, Lees WR. Multi-slice technology in computed tomography. *Clin Radiol*. 2001;56:302–9.



37. Kwong Y, Mel AO, Wheeler G, Troupis JM. Four-dimensional computed tomography (4DCT): a review of the current status and applications. *J Med Imaging Radiat Oncol*. 2015;59:545–54.
38. Taguchi K, Chiang BS, Hein IA. Direct cone-beam cardiac reconstruction algorithm with cardiac banding artifact correction. *Med Phys*. 2006;33:521–39.
39. DeRouen A, Spriet M, Aleman M. Prevalence of anatomical variation of the sixth cervical vertebra and association with vertebral canal stenosis and articular process osteoarthritis in the horses. *Vet Radiol Ultrasound*. 2016;57:253–8.
40. Birmingham SSW, Reed SM, Mattoon JS, Saville WJ. Qualitative assessment of corticosteroid cervical articular facet injection in symptomatic horses. *Equine Vet Educ*. 2010;22:77–82.
41. Pepe M, Angelone M, Gialletti R, Nannarone S, Beccati F. Arthroscopic anatomy of the equine cervical articular process joints. *Equine Vet J*. 2014;46:345–51.
42. Wang LU, Hayes S, Paskalev K, Jin L, Buyyounouski MK, Ma C-M, et al. Dosimetric comparison of stereotactic body radiotherapy using 4D CT and multiphase CT images for treatment planning of lung cancer: evaluation of the impact on daily dose coverage. *Radiother Oncol*. 2009;91:314–24.
43. Numata S, Tsutsumi Y, Monta O, Yamazaki S, Seo H, Yoshida S, et al. Mechanical valve evaluation with four-dimensional computed tomography. *J Heart Valve Dis*. 2013;22:837–42.
44. Suzuki K, Morita S, Masukawa AI, Machida H, Ueno E. Diagnosing a large slowly enhanced cerebral aneurysm using four-dimensional multiphase dynamic contrast-enhanced computed tomography angiography. *Jpn J Radiol*. 2010;28:680–3.
45. Gasiorowski JC, Richardson DW. Clinical use of computed tomography and surface markers to assist internal fixation within the equine hoof. *Vet Surg*. 2015;44:214–22.
46. Puchalski SM, Galuppo LD, Hornof WJ, Wisner ER. Intraarterial contrast-enhanced computed tomography of the equine distal extremity. *Vet Radiol Ultrasound*. 2007;48:21–9.
47. Jackson MA, Ohlerth S, Fürst AE. Use of an aiming device and computed tomography for assisted debridement of subchondral cystic lesions in the limbs of horses. *Vet Surg*. 2019;48:O15–24.
48. Mageed M. Standing computed tomography of the equine limb using a multi-slice helical scanner: technique and feasibility study. *Equine Vet Educ*. 2021;34(2):77–83. <https://doi.org/10.1111/eve.13388>
49. Sleutjens J, Cooley AJ, Sampson SN, Wijnberg ID, Back W, van der Kolk JH, et al. The equine cervical spine: comparing MRI and contrast-enhanced CT images with anatomic slices in the sagittal, dorsal, and transverse plane. *Vet Q*. 2014;34:74–84.

## SUPPORTING INFORMATION

Additional supporting information may be found in the online version of the article at the publisher's website.

**How to cite this article:** Schulze N, Werpy N, Gernhardt J, Fritsch G, Hildebrandt T, Vanderperren K, et al. Dynamic three-dimensional computed tomographic imaging facilitates evaluation of the equine cervical articular process joint in motion. *Equine Vet J*. 2023;55(1):83–91. doi:[10.1111/evej.13560](https://doi.org/10.1111/evej.13560)